International Journal of Biochemistry and Cell Biology 117 (2019) 105635

Contents lists available at ScienceDirect

International Journal of Biochemistry and Cell Biology

journal homepage: www.elsevier.com/locate/biocel

NAD$^+$ repletion inhibits the endothelial-to-mesenchymal transition induced by TGF-β in endothelial cells through improving mitochondrial unfolded protein response

Minxue Zhang[a], Haixu Weng[b], Juke Zheng[a,*]

[a] Departments of Cardiology, The Third Affiliated Hospital of Wenzhou Medical University, Wenzhou 325200, PR China
[b] ICU, The Third Affiliated Hospital of Wenzhou Medical University, Wenzhou 325200, PR China

ARTICLE INFO

Keywords:
Nicotinamide riboside
Mitochondrial unfolded protein response
Endothelial-mesenchymal transition
Prohibitin proteins
Endothelial cells

ABSTRACT

Endothelial-to-mesenchymal transition (EndMT) plays an important role in the progression of cardiac fibrosis but its mechanism and treatment need to be further understood. Herein, we have found that mitochondrial unfolded protein response (mtUPR) played a critical role in transforming growth factor beta 1 (TGF-β1)-induced EndMT in endothelial cells (ECs). MtUPR was repressed in endothelial cells after exposure to TGF-β1. NAD + precursor nicotinamide riboside (NR) could attenuate TGF-β1-induced EndMT and improve the levels of mtUPR. Significantly, prohibitin proteins (PHB and PHB2) was also regulated by nicotinamide riboside. Moreover, we found that inhibition of prohibitin proteins could prevent the protective effect of nicotinamide riboside on mtUPR and TGF-β1-induced EndMT. Overexpression of prohibitin proteins could alleviate mitochondrial function and TGF-β1-induced EndMT through improving mtUPR. In vivo, The EndMT of ECs induced by Transverse aortic constriction (TAC) in mouse was inhibited by NR. In conclusion, our results indicate that nicotinamide riboside improved the expression of prohibitin proteins to ameliorate EndMT via promotion of mtUPR. Nicotinamide riboside is a potential therapeutic target for cardiac fibrosis.

1. Introduction

As a devastating disease, heart failure (HF) is mainly induced by cardiac fibrosis (CF) and cause worldwide death (Gonzalez et al., 2018). However, the mechanism of cardiac fibrosis remains unknown. The main cellular mediator of cardiac CF is considered to be fibroblasts, until now, little was known for us about the origin of newly formed fibroblasts (Zeisberg and Kalluri, 2010). It is reported that fibroblast accumulation originates from epithelial cells due to epithelial-mesenchymal transition (EMT).

Endothelial cells (ECs) lose specific markers including E-cadherin, CD31, vWF and so on, obtain a myofibroblast or mesenchymal phenotype and express mesenchymal specific markers including Vimentin, α-smooth muscle actin (α-SMA), fibroblast specific protein 1 (FSP-1), fibronectin and so on that appeared to be characteristic of endothelial–mesenchymal transition (EndMT) (Li et al., 2018). ECs acquired mesenchymal specific markers manifest migratory, invasive, and organization to cause a striking change in cell morphology that forms elongated, spindle-shaped cells (Arciniegas et al., 2007; Kitao et al., 2009). Previous studies reported that EndMT, which could be observed in various stages of cardiovascular development, is a critical process of embryonic cardiac development (Hao et al., 2019), but recent studies have reported that it was a major pathological change in CF and pulmonary arterial hypertension (Xu et al., 2015a; Hopper et al., 2016). However, little is known about the signaling mechanisms that induce endothelial cells to transform into mesenchymal cells. A lot of treatments can cause EndMT such as hypoxia, transforming growth factor-β (TGF-β), high glucose, inflammation and radiation (Xu et al., 2015b; Zeisberg et al., 2007). All of pathways can induce the expression of transcription factors such as Snail, Slug and so on, thereby inducing the repression of endothelial genes and/or expression of mesenchymal genes (Gonzalez and Medici, 2014).

As a transcriptional response, mitochondrial unfolded protein response (mtUPR) is induced by multiple forms of mitochondrial dysfunction (Schulz and Haynes, 2015). There is a strong evidence that mitochondrial dysfunction is one of the important hallmarks in organismal aging diseases (Durieux et al., 2011; Kuilman et al., 2010; Macedo et al., 2017). Mitochondrial dysfunction can be caused by

* Corresponding author at: Department of Cardiology, The Third Affiliated Hospital of Wenzhou Medical University, 108 Wansong Road, Rui'an, Wenzhou 325200, PR China.
E-mail address: zhengjuke2008@126.com (J. Zheng).

https://doi.org/10.1016/j.biocel.2019.105635
Received 12 July 2019; Received in revised form 3 October 2019; Accepted 14 October 2019
Available online 15 October 2019
1357-2725/ © 2019 Elsevier Ltd. All rights reserved.

Table 1
Primers used for qPCR.

Gene	Forward 5'-3'	Reverse 5'-3'
CD31	GCGAGTCATGGCCCGAAGGC	GGTGGTGCTGACATCCGCGA
vWF	TTGACGGGGAGGTGAATGTG	ATGTCTGCTTCAGGACCACG
α-SMA	CTATGAGGGCTATGCCTTGCC	GCTCAGCCAGTAGTAACGAAGGA
Vimentin	GCAAAGATTCCACTTTGCGT	GAAATTGCAGGAGGAGATGC
CDH5	AAAGAATCCATTGTGCAAGTCC	CGTGTTATCGTGATTATCCGTG
ACTA2	CTCGTGTGCGACAATGGCTC	CGTCGCCCACGTAGGAATCT
FSP1	TGATGAGCAACTTGGACAGCAACAG	CGTCGGCCCACGTAGGAATCT
HSP10	CTGACAGGTTCAATCTCTCCAC	AGGTGGCATTATGCTTCCAG
HSP60	ACAGTCCTTCGCCAGATGAGAC	TGGATTAGCCCCTTTGCTGA
LONP1	TATGGAGATGATCAACGTGTCG	GACAATCTTGTAGGCCGATTTC
PHB	TCGGGAAGGAGTTCACAGAG	CAGCCTTTTCCACCACAAAT
PHB2	CACAGAGCCATCTTCTTCAATC	GGTTGTCAGCTGTGAGATAGAT
N-cadherin	CAACTTGCCAGAAAACTCCAGG	ATGAAACCGGGCTATCTGCTC
GAPDH	GAAGGTGAAGGTCGGAGTC	GAAGATGGTGATGGGATTTC

depletion of nicotinamide adenine dinucleotide (NAD+). Previous studies have verified that mtUPR deficiency is associated with many age-induced diseases including Parkinson, Alzheimer, hereditary spastic paraplegia and Friedreich ataxia (De Mena et al., 2009; Hansen et al., 2002; Guillon et al., 2009). It is regrettable that the role of mtUPR in EndMT still remains unclear.

NAD^+ deficiency is considered as a common contributor to age-related disease (Gomes et al., 2013). Recent studies have reported that supplemental NAD + precursors such as nicotinamide riboside (NR), nicotinamide mononucleotide and niacin can ameliorate a big amount of age-induced cellular impairments (Zhang et al., 2016; Hosseini et al., 2019). Nicotinamide adenine dinucleotide also acts a pivotal role in age-related vascular dysfunction (Csicsar et al., 2019). Many enzymes expressed abundantly in endothelial cells require to metabolize NAD^+ precursors, suggesting that endothelial NAD^+ levels are increased through supplemental NAD^+ precursors (Yoshino et al., 2018). Therefore, we hypothesize that nicotinamide riboside (NR), a NAD^+ precursors, can alleviate TGF-β-induced EndMT to ameliorate cardiac fibrosis through regulating mitochondrial unfolded protein response.

The purpose of this paper aims to clarify the role of NAD + precursor nicotinamide riboside in myocardial fibrosis and to elucidate the mechanism of mitochondrial unfolded protein response in this process. Our study illustrates the role of mtUPR in cardiac fibrosis and demonstrate NAD + precursor nicotinamide riboside is able to attenuate the TGF-β-induced EndMT in cardiac fibrosis. Our research also provides a new potential therapeutic strategy for myocardial fibrosis.

2. Materials and methods

2.1. Cell culture

Primary human umbilical vein endothelial cells (HUVECs) were harvested from human umbilical cord veins and cultivated with the EGM-2 bullet kit (Lonza, Basel, Switzerland) at 37℃ in 5% CO_2 in a humidified atmosphere. Experiments were performed in HUVECs between passages two and six. Human microvascular endothelial cells (HMECs) were obtained from Lonza and cultivated in EGM-2 media with supplements according to previous study (Zhang et al., 2016). ECs (endothelial cells) were exposed to TGF-β1 (10 ng/ml; Peprotech) in serum-free medium for 48 h to induced EndMT.

2.2. Animal model and surgery

Transverse aortic constriction (TAC) was performed in male C57BL/6 wild type mice (6–8 weeks old) under anesthesia intraperitoneally using pentobarbital sodium (50 mg/kg) according to previous study (Li et al., 2016). Mice were randomly assigned to Sham-operated groups, TAC groups and TAC + NR groups. Adequacy of anesthesia was assessed by documenting heart rate and observing muscle twitch and by tail pinch as well as body temperature. In order to induce aortic stenosis, a trans-sternal thoracotomy was carried out, a 27-gauge desharpened needle was placed along the thoracic aorta, followed by a tight banding of both aorta through needle with a 7-0 silk thread. The needle was withdrawn and left a stenosis in the aortic lumen. Sham-operated mice were performed with the same procedure without aortic constriction. Mice were fed with pellets containing vehicle or NR (400 mg/kg/day) for 6–8 weeks. Animal studies were approved by the Animal Care and Use Committee of The Third Affiliated Hospital of Wenzhou Medical University and all animal experiments were complied with the ARRIVE guidelines and performed in accordance with the National Institutes of Health guide for the care and use of Laboratory animals.

2.3. Immunohistochemistry

Left ventricle (LV) from mice was fixed with 4% phosphate-buffered formalin. Samples were then paraffin embedded and serial sectioned with a microtome (4 μM). Immunohistochemistry for PHB, PHB2, CD31 and Vimentin was carried out by using anti-PHB antibody (Proteintech, 10787-1-AP, 1:200, USA), anti-PHB2 antibody (Proteintech, 12295-1-AP, 1:300, USA), anti-CD31 antibody (Proteintech, 28083-1-AP, 1:500, USA) and anti-Vimentin antibody (Proteintech, 60330-1-Ig, 1:2000, USA) overnight at 4℃. Finally, HRP-conjugate secondary antibody (Santa Cruz Biotechnology, Dallas, TX, USA) were performed to incubate the sections. After counterstaining with hematoxylin, the sections were observed in microscope.

2.4. Quantitative real-time PCR

Total RNA was extracted from ECs by using TRIzol (Takara, China) according to manufacturer's protocol. For mRNA analyzes, the reverse transcription and RT-PCR reactions were performed respectively by using a first strand complementary DNA (cDNA) reverse transcription Kit and SYBR Green/ROX qPCR Master Mix kit according to the manufacturer's protocols (Takara, Otsu, Japan). The relative mRNA expression was determined using ΔΔCt method with GAPDH as a reference gene. Table 1 showed all primer sequences.

2.5. Western blotting

Total proteins from ECs were extracted using radioimmunoprecipitation assay (RIPA) lysis buffer (Thermo Scientific, Waltham, MA#89,901) supplemented with Protease and Phosphatase Inhibitor Cocktail (Thermo Scientific #78,447) and quantified by the bicinchoninic acid (BCA) protein assay kit (Thermo Scientific #23,225). Then proteins were separated SDS-polyacrylamide gel electrophoresis

(Beyotime) and electrophoretically transferred to polyvinylidene fluoride membrane (Millipore). After being blocked with 5% skim milk, membranes were incubated with primary antibodies for CD31 (Abcam, ab24590), Vimentin (Abcam, ab92547), E-cadherin (Abcam, ab33168), α-SMA (Abcam, ab21027), FSP1(Abcam, ab124805), HSP60(Abcam, ab190828), HSP10(Signalway Antibody, 33405-1), vWF(Abcam, ab218333), PHB(Abcam, ab224653), PHB2(Proteintech, 12295-1-AP) and GAPDH (Abcam, ab181602) overnight at 4℃. Next, membranes were incubated with appropriate secondary antibodies. Proteins were visualized by using ECL reagents (Thermo).

2.6. Lentivirus transfection

Prohibitin-targeted short hairpin RNAs (shRNAs) were designed according to previous study (Zhang et al., 2016) and synthesized by GenePharma, China. The recombinant lentivirus of shPhb1&2 and control lentivirus (shNC) were synthesized prepared by GenePharma, China. The LV3-pGLV-H1 + Puro plasmids with pcDNA-Phb1&2 or control oligonucleotides (Lenti-Phb1&2 and Lenti-NC) were designed according to previous study (Zhang et al., 2016) and synthesized by GennPharma, China. Briefly, primary HUVECs and HMECs were infected with Lentivirus particle according to the manufacturer's instruction. The expression levels of PHB and PHB2 were determined by qRT-PCR and Western blotting.

2.7. Immunofluorescence staining

HUVECs were fixed with 4% paraformaldehyde for 20 min and permeabilized with 0.1% Triton-X100 in phosphate-buffered saline (PBS) for 10 min. Next, cells were blocked with 5% bovine serum albumin (BSA) for 1 h and then incubated with primary antibody HSP10 (Signalway Antibody, 33405-1,1:250), HSP60(Abcam, ab190828,1:200), CD31 (Abcam, ab24590,1:200), vWF (Abcam, ab201336, 1 μg/ml) and Vimentin (Abcam, ab45939, 1 μg/ml) overnight at 4℃. Subsequently, cells were incubated with appropriate secondary antibodies (Alexa Fluor® 488-conjugated goat antirabbit IgG H& L for vimentin, Alexa Fluor® 647-conjugated goat anti-mouse IgG H&L for CD31 and vWF) at room temperature for 1 h. Immunofluorescence was visualized using fluorescence microscopy (Olympus BX51).

2.8. Migration assay

Migration assays were performed by using transwell chambers (24-well transwell plates, Corning, USA). 1 × 105 + + cells were resuspended in the upper chamber with EGM-2 serum-free medium. Complete culture medium was added in the lower chamber and cells were incubated for 24 h. Nonmobile cells were removed, the cells below the membrane were fixed by methanol and then stained with 0.1% crystal violet for 15 min. Five randomly chosen fields were counted for each well.

2.9. Wound healing assay

About 1 × 106 + + HUVECs were seeded in six-well plates at 37℃ in 5% CO_2 in a humidified atmosphere. HUVECs reached an appropriate confluence and then wounds were scratched in cell monolayers by 10 μl plastic pipette tip. Next, HUVECs were incubated in fresh medium containing 1% FBS, TGF-β1 and NR for 48 h. Photographs were taken to evaluate the migration of HUVECs.

2.10. NAD^+ and NADH quantification

After being treated with TGF-β1 and NR, about 1 × 106 + + HUVECs incubated in six-well plates were lysed with 200 μl of lysis buffer provided by the NAD + /NADH assay kit (Biovision, k337-100). NAD + and NADH concentrations were detected according to the manufacturer's instructions. Results were analyzed according to the standard curve created by using NADH standards from the kit. NAD + and NADH concentrations of each sample were normalized to the total cell number.

2.11. Oxygen consumption rates

Oxygen consumption rates (OCR) were detected by using the Seahorse extracellular flux bioanalyzer (XF96, Seahorse Bioscience Inc.) according to previous study. 5μM of FCCP was used to uncouple mitochondria after a basal respiration. All measurements were carried out in triplicates and at least three times. Results were normalized to total cell number.

2.12. ATP measurement

HUVECs seeded in the six-well plates were lysed with 200 μl of lysis buffer provided by ATP Assay Kit (Beyotime, China). After a few min, lysate containing cells was centrifuged with 12,000 *g* at 4℃ for 5 min and then supernatant was reserved. ATP of supernatant was measured according to manufacturer's instruction. Results were analyzed according to the standard curve created by using ATP standards from the kit.

2.13. Mitochondrial staining

Mitochondrial staining was carried out according to previous described (Huang et al., 2019). Briefly, HUVECs were seeded onto coverslips with 0.01% (wt/vol) poly-L-lysine. After the treatment of TGF-β1, cells were stained with MitoTracker red (Molecular Probes) at 37 ℃ for 30 min. DAPI was used to stain nuclei. And then, we imaged the mitochondria with a microscope (Olympus, Japan).

2.14. Statistical analysis

All data displayed as histograms were presented as means ± SD (standard deviation). All statistical analysis was performed by using GraphPad Prism software. Comparisons between two groups was analyzed by Student's *t*-test and the statistical significance was showed by P value of *p < 0.05, **p < 0.01 and ***p < 0.001. For multiple comparisons, a two-way analysis of variance (ANOVA) was performed followed by a Tukey post-hoc test. The statistical significance was showed by P value of nsp ≥ 0.05, *p < 0.05, **p < 0.01 and ***p < 0.001. Other demonstrations are described in each figure legend.

3. Results

3.1. TGF-β1 induces EndMT in primary HUVECs

To evaluate the effect of TGF-β1 on EndMT in primary HUVECs, primary HUVECs were exposed to TGF-β1 (10 ng/ml) for 48 h. TGF-β1 induced an obvious EndMT alteration that the cellular morphology of HUVECs was from a polygonal, cobblestone-like shape to a more spindle-like, fibroblast shape (Fig. 1A). The results of double fluorescence staining showed that the expression of the fibroblast marker Vimentin was increased and the EC marker vWF was reduced after the HUVECs treated with TGV-β1, indicating the HUVECs underwent EndMT alteration (Fig. 1B). Quantitative real-time PCR (qRT-PCR) confirmed above observations. The messenger RNA (mRNA) levels of FSP1, Vimentin, N-cadherin and ACTA2 were increased, and CD31, CDH5 and vWF were decreased in HUVECs after TGF-β1 treatment (Fig. 1C and Fig. S1A). The outcomes of Western blotting also verified these observations. In the presence of TGF-β1, the protein expression of EC marker CD31 and E-cadherin were reduced and the fibroblast marker Vimentin and N-cadherin were increased (Fig. 1D and Fig. S1B).

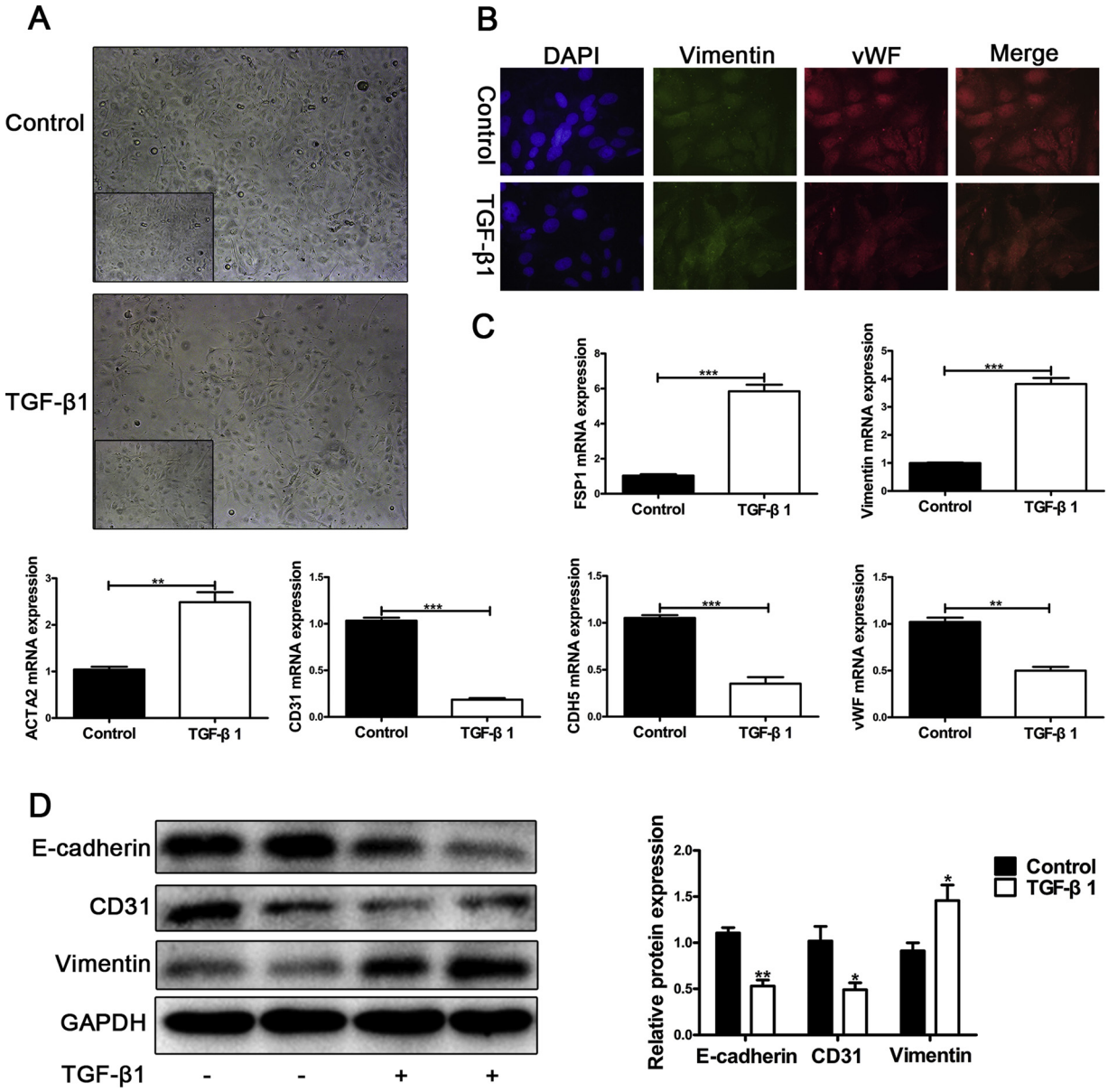

Fig. 1. Mitochondrial unfolded protein response is involved in TGF-β1-induced EndMT in cultured primary HUVECs. (A) The shape of primary HUVECs in basal media or containing TGF-β1 (10 ng/ml) for 48 h. Typical cobblestone morphology of primary HUVECs in control (basal media) versus a fibroblast-like phenotype in primary HUVECs exposed to TGF-β1. Scale Bar = 200 μm. (B) The expression of endothelial cells (ECs) marker vWF (red) and fibroblasts markers Vimentin (green) in primary HUVECs were detected by immunofluorescence. Scale Bar = 50 μm. (C) Relative mRNA expression levels of mesenchymal/myofibroblastic cells markers FSP1, Vimentin and ACTA2 and ECs markers CD31, CDH5 and vWF were determined by qRT-PCR. (D) The protein expression levels of CD31, E-cadherin and Vimentin were detected by Western blotting. All Data were presented as mean ± SEM. *$p < 0.05$, **$p < 0.01$: and ***$p < 0.001$ versus corresponding Control group. All experiments were performed at least three times. HUVECs: human umbilical vein endothelial cells; TGF-β1: transforming growth factor beta1; α-SMA: α-smooth muscle actin; EndMT: endothelial–mesenchymal transition; FSP1: fibroblastspecific protein-1; mRNA: messenger RNA; qRT-PCR: quantitative real-time polymerase chain reaction. (For interpretation of the references to colour in this figure legend, the reader is referred to the web version of this article).

These results revealed that TGF-β1 induced the EndMT in primary HUVECs.

3.2. TGF-β1 inhibits mitochondrial unfolded protein response in HUVECs

To investigate the role of mtUPR in TGF-β1-induced EndMT, we detected the level of mtUPR in HUVECs treated with TGF-β1 by PCR, Western blotting and immunofluorescence. The results of qRT-PCR showed that the mtUPR marker HSP10 and HSP60 mRNA were reduced in the presence of TGF-β1 (Fig. 2A and B). The protein level of mtUPR marker HSP10 and HSP60 were also reduced in TGF-β1-treated HUVECs (Fig. 2C). The results of immunofluorescence verified these phenomenon (Fig. 2D). To investigate the mitochondrial metabolism in TGF-β1-treated HUVECs, we measured the oxygen consumption rate (OCR) and ATP production. The OCR and ATP were reduced in primary HUVECs treated with TGF-β1 (Fig. 2E and F). The results of Mito-Tracker Red staining showed that mitochondria located in the peripheral cytoskeleton support increased velocities of directional cell migration after TGF-β1 treatment (Fig. 2G). Above results indicated that mitochondrial unfolded protein response might involve in TGF-β1-induced EndMT.

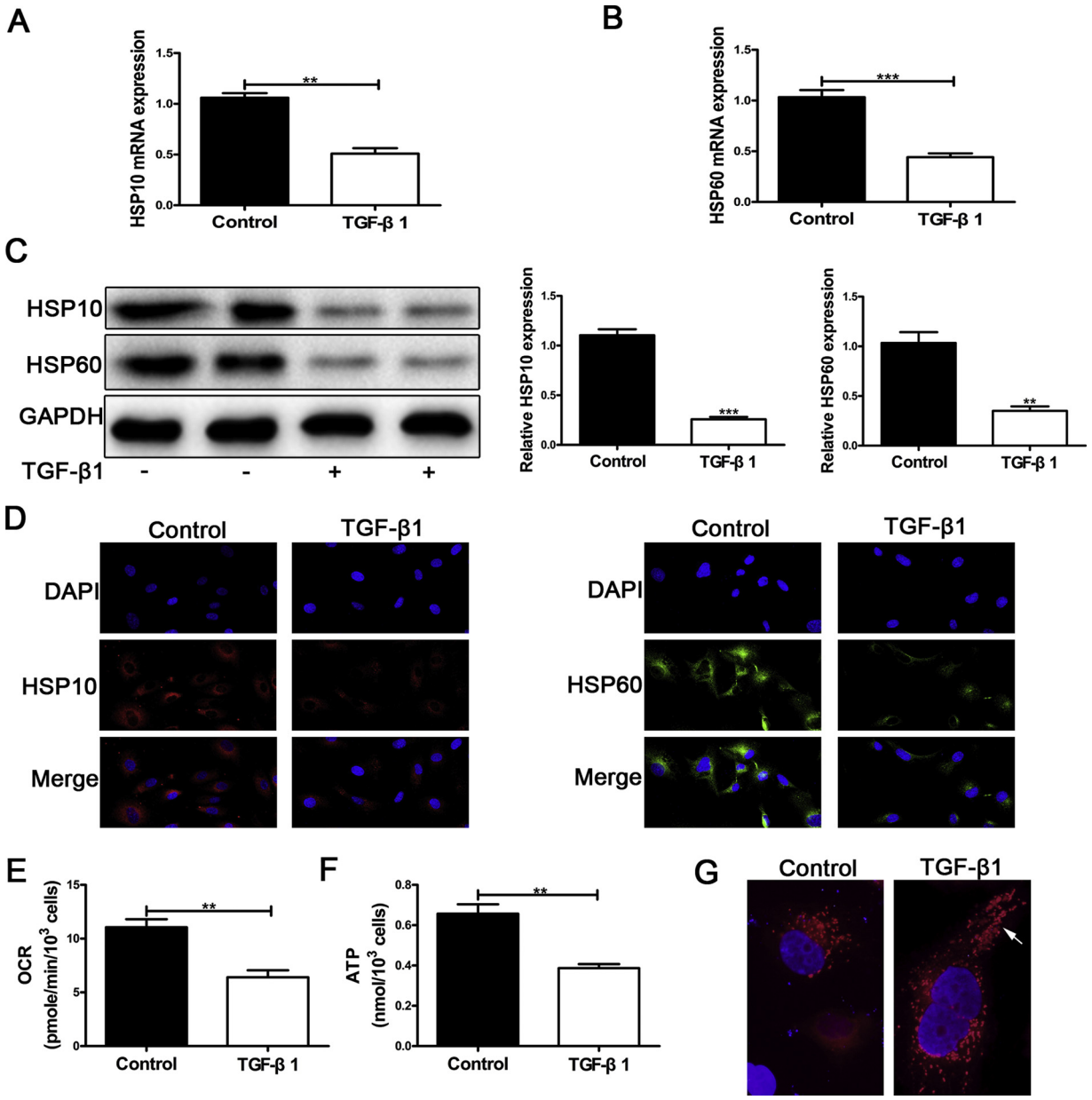

Fig. 2. TGF-β1 inhibits the levels of mtUPR in HUVECs.
(A–B) Relative mRNA expression levels of mtUPR marker HSP10 and HSP60. (C) The protein expression levels of mtUPR marker HSP10 and HSP60 were detected by Western blotting. (D) The expression of mtUPR marker HSP10 and HSP60 in primary HUVECs were detected by immunofluorescence. Scale Bar = 20 μm. (E) Oxygen consumption rate (OCR) in primary HUVECs cultured in basal media or following exposure to TGF-β1 at 37 °C. Pmole, picomoles. (F) ATP production in primary HUVECs cultured in basal media versus following exposure to TGF-β1. (G) Representative images of the mitochondrial morphology stained by MitoTracker Red. All Data were presented as mean ± SEM. *$p < 0.05$, **$p < 0.01$: and ***$p < 0.001$ versus corresponding Control group. All experiments were performed at least three times.

3.3. NR treatment can alleviate TGF-β1-induced EndMT by promotion of mtUPR in HUVECs

To investigate whether promotion of mtUPR can alleviate TGF-β1-induced EndMT, NAD^+ precursor niacinamide ribose (NR) was used to induce the mitochondrial unfolded protein response in primary HUVECs. Fig. 3A manifested that the production of NAD^+ was increased after treatment of NR. Quantitative real-time PCR (qRT-PCR) showed the mRNA of HSP60 and HSP10 were increased remarkably compared with TGF-β1 group (Fig. 3B). Western blotting confirmed that NR treatment induced an increase protein expression of HSP60 and HSP10 (Fig. 3D). The mtUPR was significant to maintain mitochondrial metabolism. Thus, we detected the OCR and ATP production of primary HUVECs and NR treatment enhanced the OCR and ATP production (Fig. 3E and F). These results suggested that NAD^+ precursor niacinamide ribose (NR) improved the mtUPR, OCR and ATP in HUVECs treated with TGF-β1.

Meanwhile, we analyzed gene expression of EC marker and fibroblast marker by qRT-PCT and Western blotting. As was shown in Fig. 3C, the increased expression of EC marker CD31 and vWF and the decreased expression of fibroblast marker Vimentin and α-SMA were observed in TGF-β1 + NR group, indicating that NR treatment was able to attenuate TGF-β1-induced EndMT. The results of Western blotting confirmed these observations. The protein expression of EC marker CD31 was significantly increased and fibroblast marker α-SMA was significantly decreased compared with levels in the TGF-β1 group

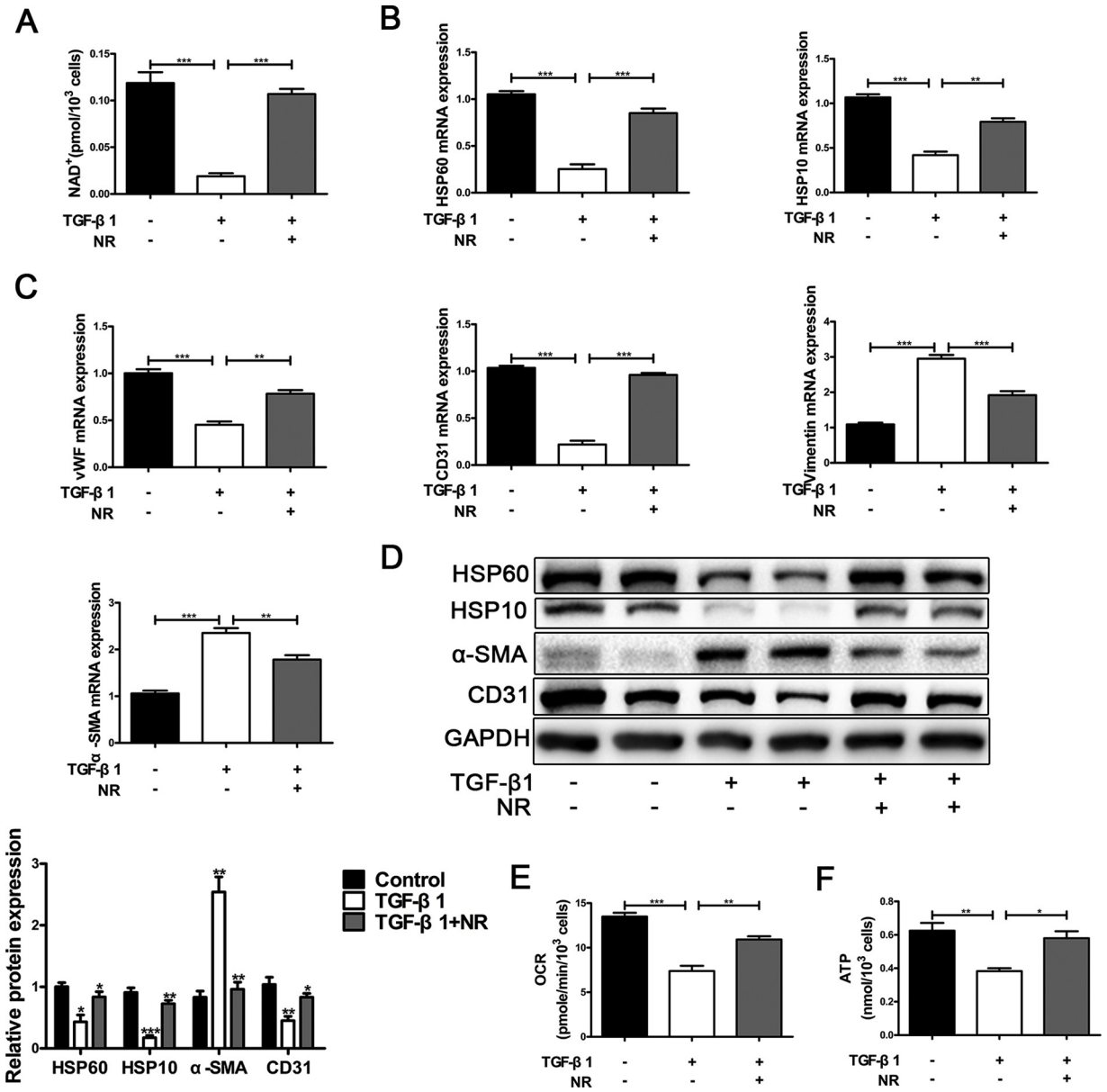

Fig. 3. NR treatment can alleviate TGF-β1-induced EndMT by promoting of mtUPR. (A) NAD + concentrations in freshly isolated HUVECs. (B) Relative mRNA expression for ECs marker genes CD31 and vWF, mesenchymal/myofibroblastic cells marker genes Vimentin, α-SMA were measured by qRT-PCR. (C) Relative mRNA expression for mtUPR genes HSP60 and HSP10 were detected by qRT-PCR. (D) The protein expression levels of HSP60, HSP10, α-SMA and CD31 were determined by Western blotting. (E) Oxygen consumption rate (OCR) in primary HUVECs at 37 °C. Pmole, picomoles. (F) ATP production in primary HUVECs. *p < 0.05, **p < 0.01 and ***p < 0.001 means statistic difference. All experiments were performed at least three times.

(Fig. 3D). These results confirmed that NR treatment could alleviate TGF-β1-induced EndMT by promoting of mtUPR.

3.4. NR treatment attenuates TGF-β1-induced EndMT in HUVECs through regulating PHB and PHB2 expression

The studies went before have reported that NR treatment promoted the mtUPR through prohibitin proteins (PHB and PHB2) (Zhang et al., 2016). The decreased expression of prohibitin proteins caused the apoptosis of ECs (Yin et al., 2015). To confirm a possible regulatory of prohibitin proteins in the NR-alleviated EndMT in ECs, we analyzed the prohibitin proteins expression in Control, TGF-1β1 and TGF-β1 + NR group in HUVECs. The quantitative qRT-PCR displayed that the mRNA of prohibitin proteins including PHB and PHB2 were decreased in TGF-β1 group and were increased in TGF-β1 + NR group (Fig. 4A). The protein expression of PHB and PHB2 were deceased in TGF-β1 group and increased in TGF-β1 + NR group (Fig. 4B). The migration of ECs was also inhibited, which showed a decrease of TGF-β1-induced EndMT, however, stand-alone NR treatment had no effect on ECs migration (Fig. 4C and D). These results revealed that NR treatment might promote the level of mtUPR and attenuate TGF-β1-induced EndMT through regulating PHB and PHB2 expression.

To further affirm the regulatory role of prohibitin proteins in HUVECs, prohibitin proteins were depleted in vitro by an shPhb1&2 lentivirus (PHB and PHB2 act only as a heterozygous protein complex) (Osman et al., 2009). The effect of shPhb1&2 lentivirus was confirmed by qRT-PCR (Fig. S1C) and Western blotting (Fig. 5A) and the results showed that PHB and PHB2 were remarkably knockdown in primary HUVECs. The alleviation of EndMT in NR-treated ECs were impaired after transfection of shPhb1&2 lentivirus. QRT-PCR and Western blotting verified this observation. As shown in Figure. S1D, a decreased mRNA expression of EC marker CD31 and an increased mRNA

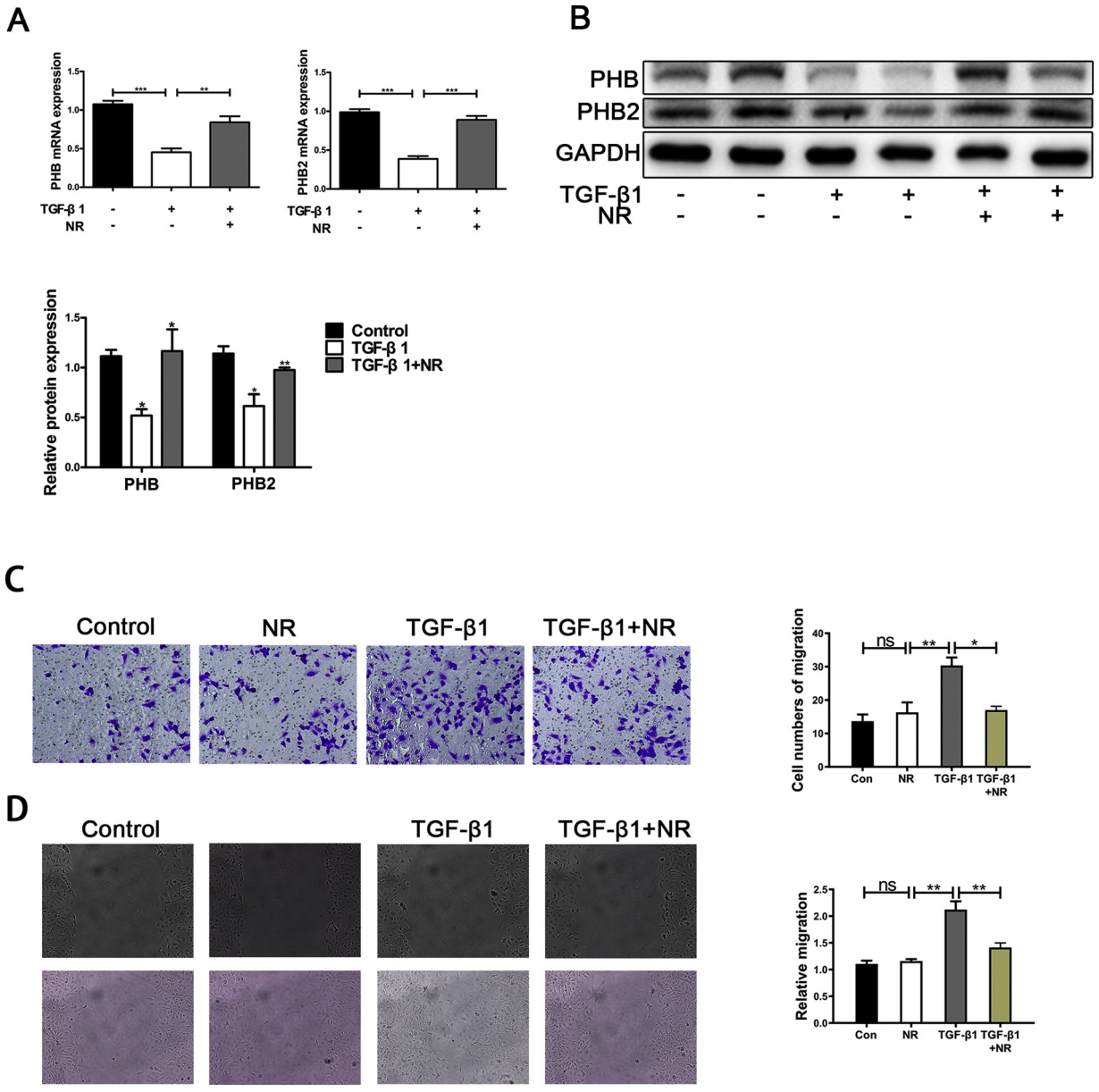

Fig. 4. NR treatment attenuates TGF-β1-induced EndMT through regulating PHB and PHB2 expression. (A) Relative mRNA expression for PHB and PHB2 were measured by qRT-PCR. (B) The protein expression levels of PHB and PHB2 were determined by Western blotting. (C) NR treatment reduced TGF-β1-induced cellular migration. Scale Bar = 50 μm. (D) Wound healing assays in primary HUVECs. Scale Bar = 50 μm. *p < 0.05, **p < 0.01 and ***p < 0.001 means statistic difference. All experiments were performed at least three times.

expression of fibroblast marker Vimentin were observed in TGF-β1 + NR + shPhb1&2 group (Fig. S1D). A decreased protein expression of EC marker CD31 and an increased protein expression of fibroblast marker Vimentin, Snail and Slug were also observed in Fig. 5C and Fig. S1E. The results of double fluorescence staining showed that expression of the fibroblast marker α-SMA (green) was decreased and the EC marker CD31 (red) was increased in HUVECs transfected with shPhb1&2, indicating the protective effect of NR was inhibited due to prohibitin proteins knockdown (Fig. 5D). These results indicated that inhibition of prohibitin proteins could block the NR-alleviated EndMT in primary HUVECs.

In order to explore whether prohibitin proteins regulate mitochondrial metabolism through mtUPR, we detected the expression of mtUPR marker HSP60, HSP10, CHOP, ATF4 and ClpP. As shown in Fig. 5B and C and Figure S1E, the mRNA expression of mtUPR marker HSP60 and HSP10 was reduced in TGF-β1 + NR + shPhb1&2 group. The protein expression of mtUPR marker HSP60, HSP10, CHOP, ATF4 and ClpP was also reduced in TGF-β1 + NR + shPhb1&2 group. OCR and ATP production to evaluate mitochondrial metabolism was also reduced in TGF-β1 + NR + shPhb1&2 group (Fig. 5E and F). These findings revealed that inhibition of prohibitin proteins could block the NR-induced mtUPR in primary HUVECs.

3.5. Overexpression of prohibitin proteins can reduce TGF-β1-induced EndMT in HUVECs

To further certify how prohibitin proteins works in NR-treated ECs, lentivirus-based Phb1&2 (Lenti-Phb1&2) were transfected into primary HUVECs. The effect of lentivirus based Phb1&2 on primary HUVECs were determined by qRT-PCR and Western blotting. The results of qRT-PCR (Fig.S2A) and Western blotting (Fig. 6A) showed that the expression of PHB and PHB2 were increased in primary HUVECs. And then, HUVECs were transfected with Lenti-Phb1&2 before exposure to TGF-β1. As shown in Figure. S2C and Fig. 6C, overexpression of Phb1&2

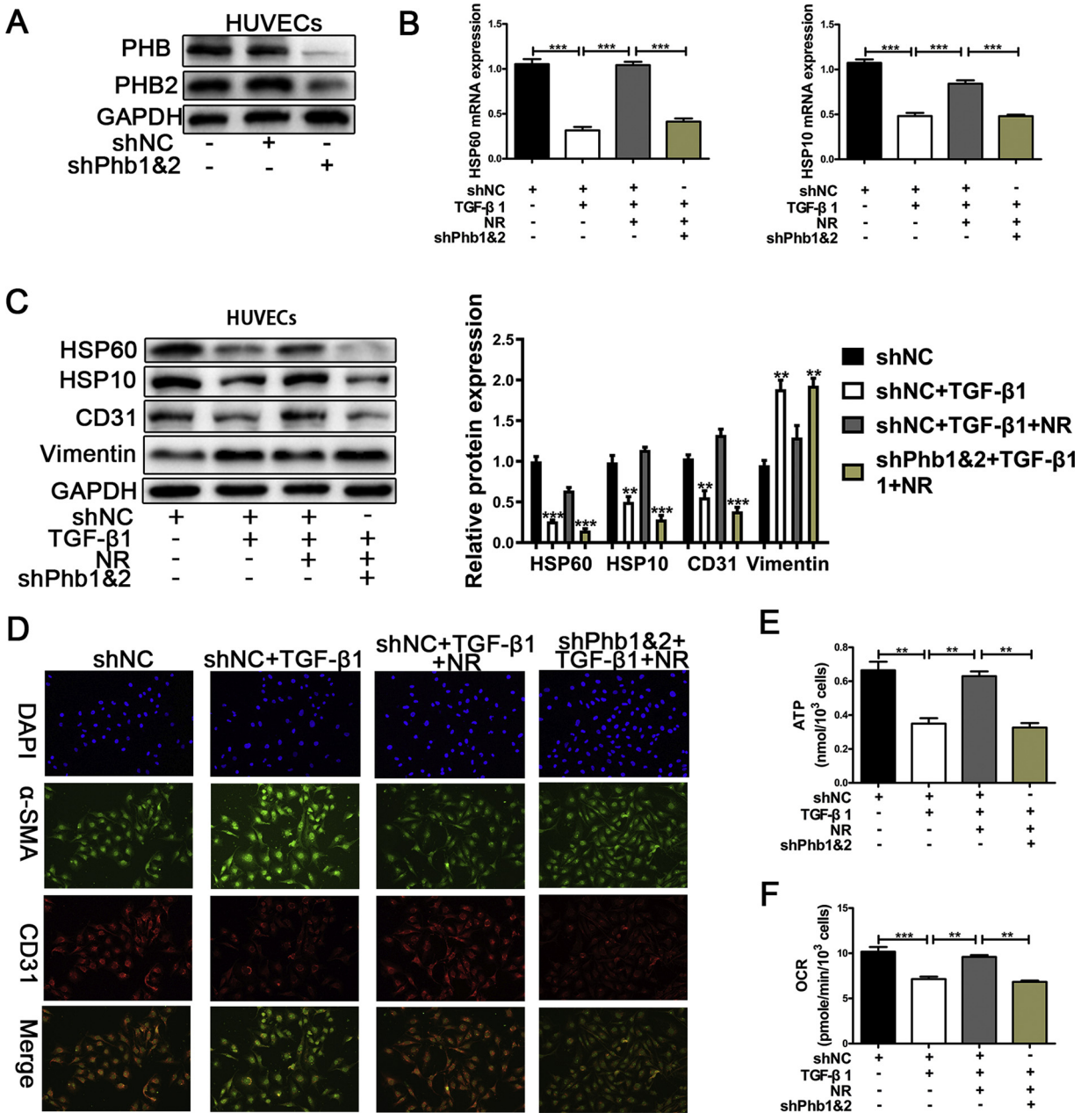

Fig. 5. Inhibition of prohibitin proteins stops the effect of NR on mtUPR, and TGF-β1 EndMT. Primary HUVECs were treated with shNC, shNC + TGF-β1, shNC + TGF-β1 + NR and shPhb1&2 + TGF-β1 + NR. (A) Effect of shPhb1&2 or shNC on primary HUVECs were determined by Western blotting. (B) The mRNA expression of HSP60 and HSP10 were detected by qRT-PCR. (C) The protein expression levels of HSP60, HSP10, CD31 and Vimentin were determined by Western blotting. (D) The expression of endothelial cells (ECs) marker CD31 (red) and fibroblasts markers α-SMA (green) were detected by immunofluorescence. Scale Bar = 50 μm. (E) ATP production in primary HUVECs. (G) Oxygen consumption rate (OCR) in primary HUVECs at 37 °C. Pmole, picomoles. *$p < 0.05$, **$p < 0.01$ and ***$p < 0.001$ means statistic difference. All experiments were performed at least three times. (For interpretation of the references to colour in this figure legend, the reader is referred to the web version of this article).

could induce an increased expression of EC marker CD31 and a decreased expression of fibroblast marker Vimentin TGF-β1 + Lenti-Phb1&2 group on mRNA and protein levels respectively. Meanwhile, we found that overexpression of Phb1&2 was able to promote the expression of mtUPR marker, OCR and ATP production in TGF-β1 + Lenti-Phb1&2 group (Figs. 6B, C, E and F and S2B and 2 D). These results suggested that overexpression of Phb1&2 could alleviate TGF-β1-induced EndMT through regulating mtUPR in HUVECs.

Sabbineni et al. have reported that TGF-β induces strong EndMT in human microvascular endothelial cells (HMECs) (Sabbineni et al., 2018). Therefore, we wanted to investigate the role of prohibitin proteins in TGF-β1-induced EndMT in HMECs. First, lentivirus-based Phb1&2 (Lenti-Phb1&2) were transfected into primary HMECs. The effect of lentivirus based Phb1&2 on HMECs were determined by qRT-PCR and Western blotting. As shown in Fig. 7A and B, the expression of PHB and PHB2 were increased in HMECs. Upregulation of Phb1&2 could cause an increased expression of EC marker CD31 and a decreased expression of fibroblast marker Vimentin in TGF-β1 + Lenti-Phb1&2 group on mRNA and protein levels respectively. Moreover, we observed that upregulation of Phb1&2 was able to promote the expression of mtUPR marker in TGF-β1 + Lenti-Phb1&2 group (Fig. 7C and D). These above results suggested that Upregulation of Phb1&2 could alleviate TGF-β1-induced EndMT through regulating mtUPR in HMECs.

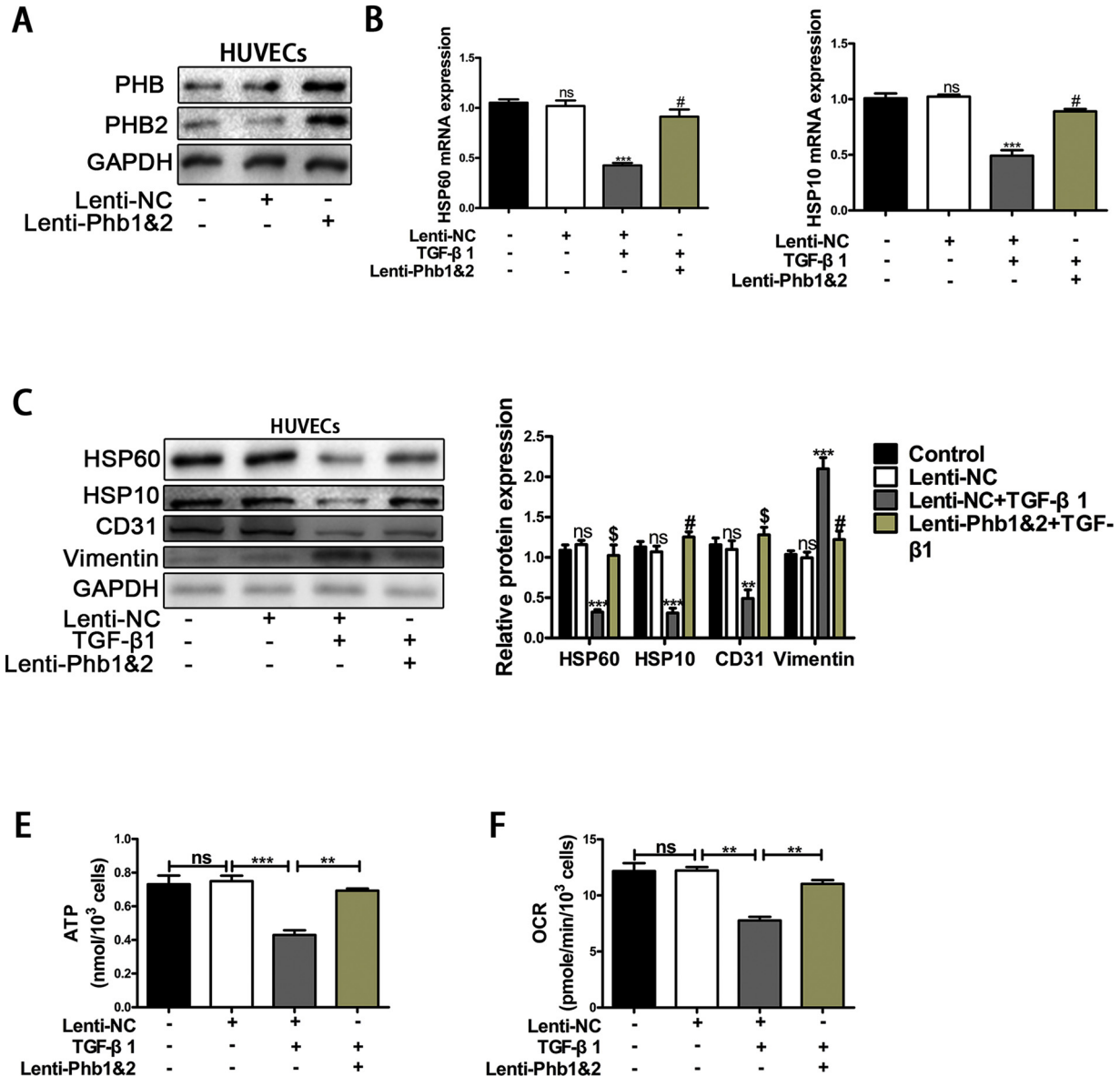

Fig. 6. Overexpression of prohibitin proteins can promote the mitochondrial unfolded protein response to attenuate TGF-β1-induced EndMT in HUVECs. Primary HUVECs were treated with control, Lenti-NC, Lenti-NC + TGF-β1 and Lenti-Phbq&2 + TGF-β1. (A) Effect of Lenti-Phb1&2 on primary HUVECs were determined by Western blotting. (B) The mRNA expression of HSP60 and HSP10 were detected by qRT-PCR. (C) The protein expression levels of HSP60, HSP10, CD31 and Vimentin were determined by Western blotting. (D) ATP production in primary HUVECs. (E) Oxygen consumption rate (OCR) in primary HUVECs at 37 °C. Pmole, picomoles. All Data were presented as mean ± SEM. nsp ≥ 0.05 versus corresponding Control group. ***p < 0.001 verses corresponding Lenti-NC group. #p < 0.001 versus corresponding TGF-β1 group in Fig. 4A; nsp ≥ 0.05, *p < 0.05, **p < 0.01 and ***p < 0.001 versus corresponding Control group.

3.6. NR treatment can repress TAC-induced EndMT by regulating prohibitin proteins expression in vivo

To investigate whether NR treatment can prevent TAC-induced EndMT, we performed a TAC procedure followed by treatment of NR from 1 day after TAC. Treatment of NR (400 mg/kg/day) for 6–8 weeks was accordance with previous study (Zhang et al., 2016). We observed that hearts of mice treated with TAC + NR had remarkably higher levels of CD31 and lower levels of Vimentin compared to TAC-treated mice (Fig. 8A). The protein expression of PHB and PHB2 were also upregulated in TAC + NR-treated mice (Fig. 8A). These above results revealed that NR treatment could repress TAC-induced EndMT by enhancing prohibitin proteins expression in vivo.

4. Discussion

Here, our study has revealed for the first time that NAD^+ repletion (NR) can ameliorate the TGF-β1-induced EndMT process through promoting the levels of mtUPR and prohibitin proteins (PHB and PHB2) acts as a mediator between NR and mtUPR. Our research provided direct evidence that TGF-β1 was able to induce EndMT and mtUPR levels were significantly downregulated in HUVECs after exposing to TGF-β1. The decreased levels of mtUPR lead to mitochondrial dysfunction. We found that NR treatment not only enhanced the levels of mtUPR and inhibited the EndMT induced by TGF-β1 but also alleviated the mitochondrial dysfunction. what's more, it is pointed out that prohibitin proteins regulated the NR-induced mtUPR. Inhibition of prohibitin proteins impaired the protective effect of NR treatment on TGF-β1-induced EndMT in ECs. In contrast, lentivirus-mediated overexpression of prihibitin proteins prevented EndMT of ECs. Importantly, NR treatment

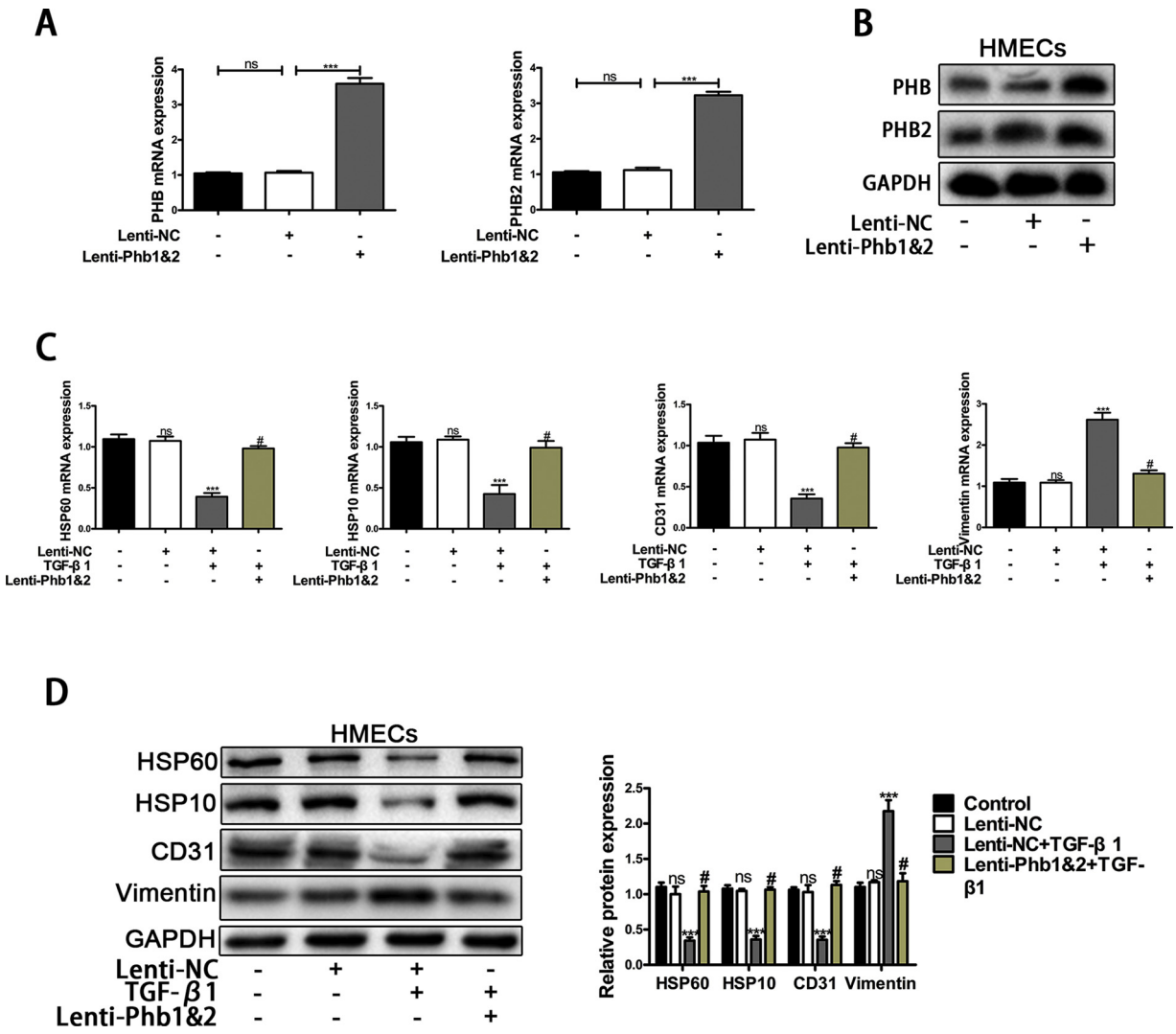

Fig. 7. Upregulation of prohibitin proteins can promote the mitochondrial unfolded protein response to attenuate TGF-β1-induced EndMT in HMECs. HMECs were treated with control, Lenti-NC, Lenti-NC + TGF-β1 and Lenti-Phbq&2 + TGF-β1. (A) Effect of Lenti-Phb1&2 or Lenti-NC on HMECs were determined by qRT-PCR. (B) Effect of Lenti-Phb1&2 on HMECs were determined by Western blotting. (C) The mRNA expression of CD31, Vimentin, HSP60 and HSP10 were detected by qRT-PCR. (D) The protein expression levels of HSP60, HSP10, CD31 and Vimentin were determined by Western blotting. All Data were presented as mean ± SEM. nsp ≥ 0.05 versus corresponding Control group. ***p < 0.001 verses corresponding Lenti-NC group. #p < 0.001 versus corresponding TGF-β1 group.

can prevent TAC-induced EndMT through promoting the expression of PHB and PHB2 in vivo, what means that NR treatment may be a potential therapeutic method to EndMT-related CF through prohibitin-regulated mtUPR.

EndMT-derived ECs are major source for myofibroblasts which counts a great deal in the pathogenesis of CF (Zeisberg et al., 2007). The changes of cell specific markers and structural rearrangements are observed in EndMT-derived ECs. EC specific markers such as CD31, vWF and so on are decreased in the process of EndMT while fibroblast specific markers such as Vimentin, α-SMA and FSP1 are increased (Cooley et al., 2014)(Fig. 1). It is known that TGF-β signaling pathway can drive EndMT in cardiac injury (Song et al., 2019). Our results confirmed that TGF-β1 was able to induce EndMT by causing a decrease of mtUPR. Mitochondrial function was damaged due to a decrease of mtUPR (Fig. 1). From the above analysis, we conclude that mtUPR is vital to TGF-β1-induced EndMT.

EndMT is a major pathogenesis factor for CF and ultimately resulted in heart failure (Gonzalez et al., 2018). mtUPR may be a potential therapeutic target for EndMT in ECs. To verify this hypothesis, NR was used to promote the levels of mtUPR. Recent studies have shown that NR can attenuate senescence by correcting mitochondrial dysfunction as a NAD^+ repletion (Michel et al., 2015). To our knowledge, our results are the first to reveal NR-alleviated EndMT in ECs. The multifaceted vasoprotective effects of NR on age-related endothelial dysfunction such as atherosclerotic vascular diseases and hypertension (Lerman and Zeiher, 2005; Ungvari et al., 2018a, b). This study performed that NR treatment reduced the expression of fibroblast specific markers such as Vimentin and α-SMA as well as enhanced the expression of EC specific markers such as CD31 and vWF after exposure to TGF-β1. The migration induced by TGF-β1 was reduced. OCR and ATP production were increased, indicating that mitochondrial dysfunctions were recovered after NR treatment (Fig. 2).

Prihibitin proteins are involved in endothelial dysfunction and regulates the levels of mtUPR, suggested a study released recently (Yin et al., 2015). To verify whether NR treatment promotes mtUPR levels through prohibitin proteins, we first determined the expression of prohibitin proteins in ECs. The expression of prohibitin proteins was decreased in ECs treated with TGF-β1 and increased after NR treatment. prohibitin proteins knockdown was able to inhibit the protective effect of NR on EMT through repressing mtUPR and exacerbated mitochondrial dysfunction. In contrast, overexpression of prohibitin proteins could ameliorate EndMT induced by TGF-β1. Furthermore,

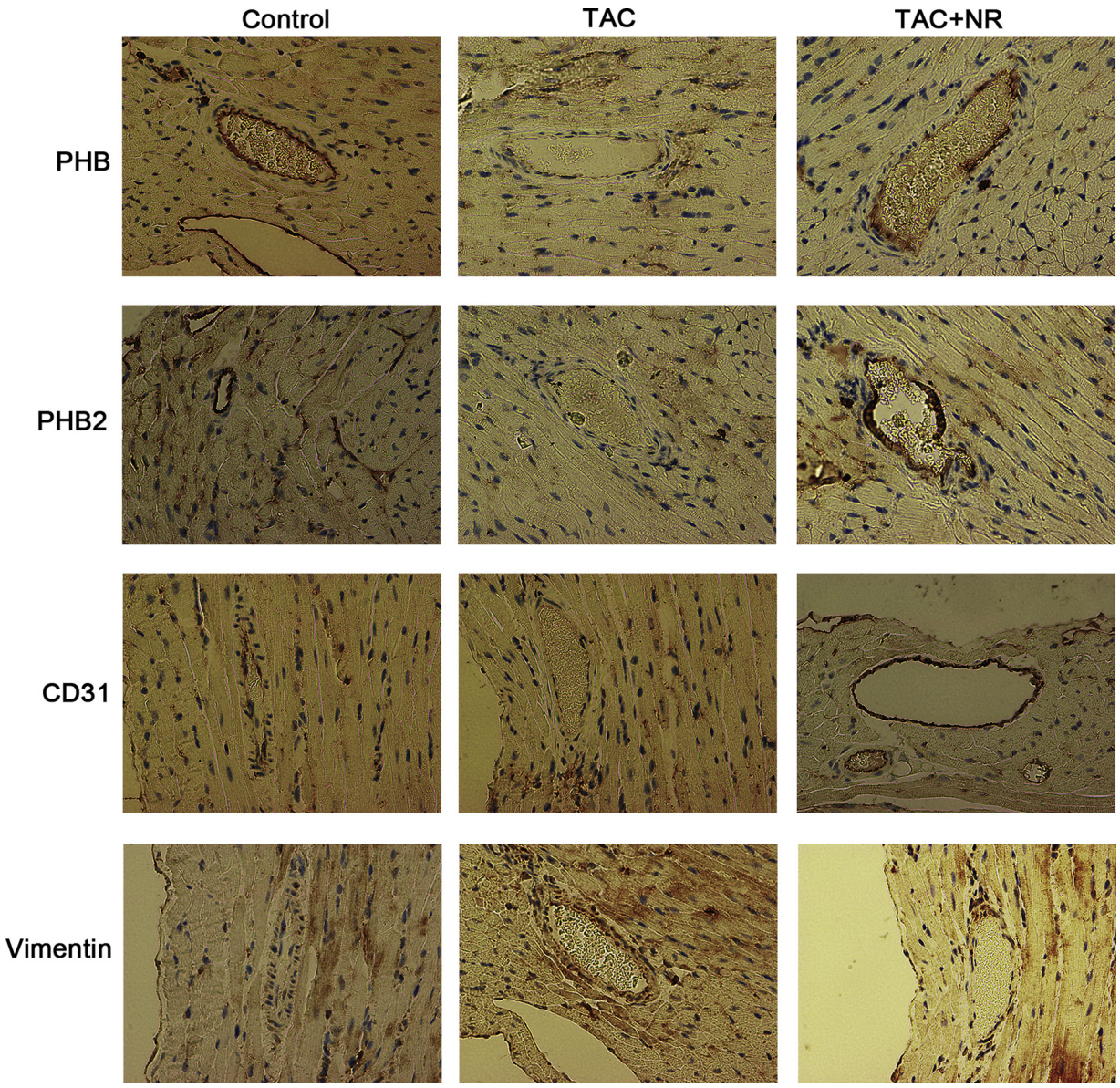

Fig. 8. NR treatment can prevent TAC-induced EndMT by enhancing PHB and PHB2 expression. (A) The protein expression of PHB, PHB2, CD31 and Vimentin in LV tissue were determined by Immunohistochemistry. All experiments were performed at least three times.

overexpression of prohibitin proteins promoted the levels of mtUPR to maintain mitochondrial function. In vivo, treatment of NR could attenuate TAC-induced EndMT by upregulating PHB and PHB2 expression. These results have suggested that NR treatment can promote the expression of prohibitin proteins to alleviate EMT through regulating mtUPR levels.

5. Conclusion

In conclusion, NR treatment facilitates the protein expression of prohibitin proteins to prevent TGF-β1-induced EndMT through regulating mtUPR. Our study provides a new therapeutic method to prevent EndMT in cardiac fibrosis.

Conflicts of interest

The authors declare that they have no competing interests.

Data availability statement

All Data in our study is availability.

Author contribution statement

Juke Zheng contributes to Working concept or design. Minxue Zhang contributes to data collection. Haixu Weng contributes to Draft paper.

Acknowledgements

Thanks to my colleagues in my lab. Their help is crucial for me to complete this article.

Appendix A. Supplementary data

Supplementary material related to this article can be found, in the online version, at doi:https://doi.org/10.1016/j.biocel.2019.105635.

References

Gonzalez, A., Schelbert, E.B., Diez, J., Butler, J., 2018. Myocardial interstitial fibrosis in heart failure: biological and translational perspectives. J. Am. Coll. Cardiol. 71, 1696–1706.

Zeisberg, E.M., Kalluri, R., 2010. Origins of cardiac fibroblasts. Circ. Res. 107, 1304–1312.

Li, Z., Wang, F., Zha, S., Cao, Q., Sheng, J., Chen, S., 2018. SIRT1 inhibits TGF-beta-induced endothelial-mesenchymal transition in human endothelial cells with Smad4 deacetylation. J. Cell. Physiol. 233, 9007–9014.

Arciniegas, E., Frid, M.G., Douglas, I.S., Stenmark, K.R., 2007. Perspectives on endothelial-to-mesenchymal transition: potential contribution to vascular remodeling in chronic pulmonary hypertension. Am. J. Physiol. Lung Cell Mol. Physiol. 293, L1–L8.

Kitao, A., Sato, Y., Sawada-Kitamura, S., et al., 2009. Endothelial to mesenchymal transition via transforming growth factor-beta1/Smad activation is associated with portal venous stenosis in idiopathic portal hypertension. Am. J. Pathol. 175, 616–626.

Hao, Y.M., Yuan, H.Q., Ren, Z., et al., 2019. Endothelial to mesenchymal transition in atherosclerotic vascular remodeling. Clin. Chim. Acta 490, 34–38.

Xu, X., Tan, X., Tampe, B., et al., 2015a. Epigenetic balance of aberrant Rasal1 promoter methylation and hydroxymethylation regulates cardiac fibrosis. Cardiovasc. Res. 105, 279–291.

Hopper, R.K., Moonen, J.R., Diebold, I., et al., 2016. In pulmonary arterial hypertension, reduced BMPR2 promotes endothelial-to-Mesenchymal transition via HMGA1 and its target slug. Circulation 133, 1783–1794.

Xu, X., Tan, X., Tampe, B., Sanchez, E., Zeisberg, M., Zeisberg, E.M., 2015b. Snail is a direct target of hypoxia-inducible factor 1alpha (HIF1alpha) in hypoxia-induced endothelial to mesenchymal transition of human coronary endothelial cells. J. Biol. Chem. 290, 16653–16664.

Zeisberg, E.M., Tarnavski, O., Zeisberg, M., et al., 2007. Endothelial-to-mesenchymal transition contributes to cardiac fibrosis. Nat. Med. 13, 952–961.

Gonzalez, D.M., Medici, D., 2014. Signaling mechanisms of the epithelial-mesenchymal transition. Sci. Signal. 7 re8.

Schulz, A.M., Haynes, C.M., 2015. UPR(mt)-mediated cytoprotection and organismal aging. Biochim. Biophys. Acta 1847, 1448–1456.

Durieux, J., Wolff, S., Dillin, A., 2011. The cell-non-autonomous nature of electron transport chain-mediated longevity. Cell 144, 79–91.

Kuilman, T., Michaloglou, C., Mooi, W.J., Peeper, D.S., 2010. The essence of senescence. Genes Dev. 24, 2463–2479.

Macedo, J.C., Vaz, S., Logarinho, E., 2017. Mitotic dysfunction associated with aging hallmarks. Adv. Exp. Med. Biol. 1002, 153–188.

De Mena, L., Coto, E., Sanchez-Ferrero, E., et al., 2009. Mutational screening of the mortalin gene (HSPA9) in Parkinson's disease. J. Neural Transm. (Vienna, Austria : 1996) 116, 1289–1293.

Hansen, J.J., Durr, A., Cournu-Rebeix, I., et al., 2002. Hereditary spastic paraplegia SPG13 is associated with a mutation in the gene encoding the mitochondrial chaperonin Hsp60. Am. J. Hum. Genet. 70, 1328–1332.

Guillon, B., Bulteau, A.L., Wattenhofer-Donze, M., et al., 2009. Frataxin deficiency causes upregulation of mitochondrial Lon and ClpP proteases and severe loss of mitochondrial Fe-S proteins. FEBS J. 276, 1036–1047.

Gomes, A.P., Price, N.L., Ling, A.J., et al., 2013. Declining NAD(+) induces a pseudo-hypoxic state disrupting nuclear-mitochondrial communication during aging. Cell 155, 1624–1638.

Zhang, H., Ryu, D., Wu, Y., et al., 2016. NAD(+) repletion improves mitochondrial and stem cell function and enhances life span in mice. Science (New York, NY) 352, 1436–1443.

Hosseini, L., Vafaee, M.S., Mahmoudi, J., Badalzadeh, R., 2019. Nicotinamide adenine dinucleotide emerges as a therapeutic target in aging and ischemic conditions. Biogerontology.

Csicsar, A., Tarantini, S., Yabluchanskiy, A., et al., 2019. Role of endothelial NAD+ deficiency in age-related vascular dysfunction. Am. J. Physiol. Heart Circ. Physiol.

Yoshino, J., Baur, J.A., Imai, S.I., 2018. NAD(+) intermediates: the biology and therapeutic potential of NMN and NR. Cell Metab. 27, 513–528.

Li, C.Y., Chen, Y.H., Wang, Q., et al., 2016. Partial inhibition of activin receptor-like kinase 4 attenuates pressure overload-induced cardiac fibrosis and improves cardiac function. J. Hypertens. 34, 1766–1777.

Huang, G., Cong, Z., Wang, X., et al., 2019. Targeting HSP90 attenuates angiotensin II-induced adventitial remodeling via suppression of mitochondrial fission. Cardiovasc. Res.

Yin, W., Li, B., Li, X., et al., 2015. Critical role of prohibitin in endothelial cell apoptosis caused by glycated low-density lipoproteins and protective effects of grape seed procyanidin B2. J. Cardiovasc. Pharmacol. 65, 13–21.

Osman, C., Merkwirth, C., Langer, T., 2009. Prohibitins and the functional compartmentalization of mitochondrial membranes. J. Cell. Sci. 122, 3823–3830.

Sabbineni, H., Verma, A., Somanath, P.R., 2018. Isoform-specific effects of transforming growth factor beta on endothelial-to-mesenchymal transition. J. Cell. Physiol. 233, 8418–8428.

Cooley, B.C., Nevado, J., Mellad, J., et al., 2014. TGF-beta signaling mediates endothelial-to-mesenchymal transition (EndMT) during vein graft remodeling. Sci. Transl. Med. 6 227ra234.

Song, S., Zhang, R., Cao, W., et al., 2019. Foxm1 is a critical driver of TGF-beta-induced EndMT in endothelial cells through Smad2/3 and binds to the Snail promoter. J. Cell. Physiol. 234, 9052–9064.

Michel, S., Canonne, M., Arnould, T., Renard, P., 2015. Inhibition of mitochondrial genome expression triggers the activation of CHOP-10 by a cell signaling dependent on the integrated stress response but not the mitochondrial unfolded protein response. Mitochondrion 21, 58–68.

Lerman, A., Zeiher, A.M., 2005. Endothelial function: cardiac events. Circulation 111, 363–368.

Ungvari, Z., Tarantini, S., Donato, A.J., Galvan, V., Csiszar, A., 2018a. Mechanisms of vascular aging. Circ. Res. 123, 849–867.

Ungvari, Z., Tarantini, S., Kiss, T., et al., 2018b. Endothelial dysfunction and angiogenesis impairment in the ageing vasculature. Nat. Rev. Cardiol. 15, 555–565.